Available online at www.sciencedirect.com

ScienceDirect

Journal of Environmental Sciences 19(2007) 1159–1165

JOURNAL OF ENVIRONMENTAL SCIENCES
ISSN 1001-0742
CN 11-2629/X
www.jesc.ac.cn

Hydrodynamic characteristics of a four-compartment periodic anaerobic baffled reactor

LIU Xiao-lei[1,2], REN Nan-qi[1,*], WAN Chun-li[1]

1. School of Municipal and Environmental Engineering, Harbin Institute of Technology, Harbin 150090, China. E-mail: nanyuanx@126.com
2. School of Water Conservancy and Environment Engineering, Changchun Institute of Technology, Changchun 130012, China

Received 6 December 2006; revised 5 January 2007; accepted 9 February 2007

Abstract

Periodic anaerobic baffled reactor (PABR) is a novel reactor based on the design concept of anaerobic baffled reactor (ABR). Residence time distribution (RTD) studies on both clean and working reactors at the same hydraulic residence time (HRT) of 2 d were carried out to investigate the dead spaces and mixing patterns in PABRs at different organic loading rates (OLRs) in various switching manners and frequencies. The results showed that the fraction of dead space in PABR was similar to that in ABR, which was low in comparison with other reactor designs. Dead space may be divided into two categories, hydraulic and biological. In RTD studies without biomass, the hydraulic dead space in the PABR run in an "every second" switching manner with $T = 2$ d was the lowest whereas that in the PABR run in a $T = \infty$ (ABR) switching manner was the highest. The same trend was obtained with the total dead space in RTD studies with biomass no matter what the OLR was. Biological dead space was the major contributor to dead space but affected decreasingly at higher OLR whichever switching manner the PABR run in. The flow patterns within the PABRs were intermediate between plug-flow and perfectly mixed under all the conditions tested.

Key words: dead space; residence time distribution; periodic anaerobic baffled reactor; anaerobic processes; wastewater treatment

Introduction

The hydrodynamics and degree of mixing that occur within a bioreactor strongly influence the extent of contact between substrate and bacteria, thus controlling mass transfer and potential reactor performance. Grobicki and Stuckey (1992) conducted a series of residence time distribution (RTD) studies by tracking the fate of an inert tracer (Li^+) in the effluent of a number of anaerobic baffled reactors (ABRs), both with and without biomass, at various hydraulic residence times (HRTs), and incorporated the data into "Dispersion" and "Tanks in Series" models previously described by Levenspiel (1972). The models provided a useful method to calculate the degree of mixing and the amount of unused volume (known as "dead space") within the reactor. The same experimental technique and analytical approach were performed to study the hydrodynamics of ABRs with changing HRTs, feed, or biomass concentration (Langenhoff *et al*., 2000), and to determine whether the rate of gas production and viscosity affected the hydrodynamics of the ABR at different temperatures (Langenhoff and Stuckey, 2000). However, there are few literature references that report the hydrodynamic characteristics of a novel reactor based on the ABR design concept, the periodic anaerobic baffled reactor (PABR) initially developed by Skiadas and Lyberatos (1998).

PABR consists of two concentric cylinders and the area between the cylinders is compartmentalized so that the reactor resembles an ABR with the compartments arranged in a circular manner in the annular region. Fig.1 shows the configuration of a four-compartment PABR. The feed enters the compartment through a port attached to the downflow section, comes up in the upflow section passing below the baffle, and then enters the next compartment through external tubes, and eventually leaves the system after passing through the upflow part of the effluent compartment. The role of the four-compartments is periodically changed by properly switching (on or off) the 12 valves of the outer tubing. For instance, when A is the feeding compartment, D will be the effluent one and valves 1, 3, 6, 9, 11 are switched on, while valves 2, 4, 5, 7, 8, 10, 12 are switched off. Likewise, whenever the feeding compartment is B, C, or D, the effluent one will be A, B or C, respectively.

In the extreme of zero switching frequency (no switching), the reactor behaves as an ABR. In the other extreme (infinite frequency), the compartments become identical so that the reactor will behave like a upflow anaerobic sludge blanket reactor (UASBR). By setting the switching frequency, a great flexibility is obtained, taking advantage of the optimal reactor configuration (UASBR, ABR,

Project supported by the Hi-Tech Research and Development Program (863) of China (No. 2002AA601310). *Corresponding author. E-mail: rnq@hit.edu.cn.

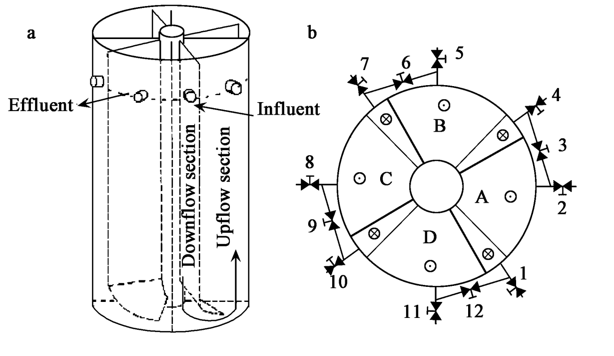

Fig. 1 Schematic diagram of the experimental device. (a) front view of a four-compartment PABR; (b) top view of a four-compartment PABR. 1, 2, ..., 12 valves positioned on tubes set outside the reactor; the external tubes connect the upflow section (⊙) of the compartment with the downflow section (⊗) of the subsequent compartment.

or "something in between") depending on the loading conditions. In addition to the switching frequency, one must decide the exact manner of switching feed and effluent compartments (clockwise, counterclockwise, every second, or sequentially etc.). For a four-compartment PABR, there are three options (when viewed from the top): "clockwise sequential", "counterclockwise sequential", and "every second". The "counterclockwise sequential" switching manner is not viable because the feeding compartment is switched to the effluent compartment whenever a switching takes place. The meaning of "clockwise sequential" switching mode is that for a given switching period (T), the order of the compartment from the influent to the effluent will be A–B–C–D if $0 < t < T/4$, D–A–B–C if $T/4 < t < T/2$, C–D–A–B if $T/2 < t < 3T/4$, and B–C–D–A if $3T/4 < t < T$. For the "every second" switching manner, the order will be A–B–C–D if $0 < t < T/2$ and C–D–A–B if $T/2 < t < T$.

Most previous studies focused on the studies of PABRs run in "clockwise sequential" switching manner. On an experimental basis, the behavior of a 15-L PABR fed with glucose was examined by Skiadas and Lyberatos (1998) at different switching periods (1, 1.5, and 2 d), but a constant organic loading rate (OLR) (4.55 kgCOD/(m^3·d)). The mean COD removal was high in all cases (> 94%). Skiadas *et al*. (2000) investigated the effect of switching frequency on PABR performance for various dilution rates and concluded that, operation of the PABR at high switching frequencies leads to higher performance for high dilution rates, while the reverse is the case for low dilution rates. Then, transient behavior of a PABR fed on gelatin or glucose under increasing organic loading conditions was explored (Stamatelatou and Lyberatos, 2002; Stamatelatou *et al*., 2003). The PABR response was satisfactory on both types of substrate, when treated separately at an OLR of 6.25 and 12.5 kgCOD/(m^3·d), respectively. Further studies of Stamatelatou *et al*. (2004) found that PABR seemed to be minimally affected during the gradual substitution of glucose by gelatin, because the reactor performance remained at an optimal level (about 98%) while operated under an OLR of 3.125 kgCOD/(m^3·d).

In this study, a series of RTD studies of three PABRs feeding with Chinese traditional medicine industrial wastewater both with and without biomass, in various switching manners and frequencies were carried out at different OLRs to analyze their hydrodynamic characteristics.

1 Materials and methods

1.1 Design of experiments

The studies were performed in three identical four-compartment PABRs made of perspex. The diameters of the two concentric cylinders and the height of each PABR with a total useful volume of 18 L were 50 mm, 250 mm, and 500 mm, respectively. The volume ratio of the downflow section to the upflow section was about 1:5 of every compartment. There were two sample ports, which were placed 100 mm both from the top of the reactor for effluent sampling and from the bottom of the reactor for sludge sampling, in the upflow section of every compartment. The produced gas was collected via portholes at the top of each compartment and was recorded using wet gas meters. The temperature of the PABR was maintained at 35°C using a strip heater twining around the outside cylinder through a temperature controller.

The RTD studies were done with clean reactor before inoculation, using only tap water (Table 1 Run a(1), b(1), c(1)). Thereafter, the reactors were seeded with sieved (0.425 mm) digester sludge from the solids treatment stage at the Harbin Brewing Group, and had a known average concentration of biomass. They were run continuously at stable HRT = 2 d, using a feed with average OLR at about 1, 2, and 4 kgCOD/(m^3·d) for 12, 24, and 24 d, respectively. During the last 6 d of feeding, with average OLR at about 2 and 4 kgCOD/(m^3·d), the RTD studies

Table 1 Design of experiments on residence time distribution (RTD) studies

Run no.	Switching manner	Switching period T (d)	Inoculation (gVSS/L)	Average OLR (kgCOD/(m^3·d))	Average COD removal (%)	Average gas production (L/d)
a(1)	Clockwise sequential	4	–		–	–
a(2)	Clockwise sequential	4	13.53	2.06	78.59	9.60
a(3)	Clockwise sequential	4	13.53	4.11	83.07	24.10
b(1)	Every second	2	–		–	–
b(2)	Every second	2	13.53	2.06	84.81	10.35
b(3)	Every second	2	13.53	4.11	91.18	22.35
c(1)	–	∞	–		–	–
c(2)	–	∞	15.44	2.06	84.81	12.98
c(3)	–	∞	15.44	4.11	91.17	23.59

were performed (Table 1, Run a(2), b(2), c(2) and Run a(3), b(3), c(3)).

1.2 Sewage

Settled sewage was a dilution of the Chinese traditional medicine industrial wastewater collected directly from the product line in the Harbin No.2 Chinese Traditional Medicine Plant. The wastewater was rich in macromolecule, which was difficult to be treated and easy to foam in aerobic biodegradation, such as glycosides. Chemical oxygen demand (COD) concentration in the wastewater ranged from 143682.2 to 586479.8 mg/L, and could be diluted to any required strength. The pH value of the wastewater was 6.75–7.54 and $NaHCO_3$ was added to the dilution with a concentration of 1.5 g$NaHCO_3$/L to maintain the alkalinity concentration (as $CaCO_3$) of 1000–1500 mg/L in the feed. BOD/COD fluctuated between 0.32 and 0.37 in both the wastewater and the dilution, whereas the COD:TN:TP remained about 258:3:1.

1.3 Sampling and analyses

The experiments to study RTD were done with an impulse, i. e., an injection of 10 ml of a lithium chloride solution (10 g Li^+/L) just before the inlet of the reactor. The concentration of lithium in the effluent was measured using an inductively coupled plasma (ICP) optical emission spectrometer (Optima 5300 DV, PerkinElmer, USA) for at least 3 HRTs after the addition of the pulse. Effluent samples were taken at regularly-spaced intervals.

All items on the quality of the influent and effluent, together with the mixed liquor volatile suspended solids (VSS) were measured according to the standard methods (American Public Health Association, 1995).

2 Results and discussion

In an RTD study, the mass balance for Li^+ can be expressed as:

$$M = \int_0^\infty v_0 C_A \mathrm{d}t \tag{1}$$

where, t is the time, M is the mass of Li^+ injected at $t = 0$, C_A is the Li^+ concentration in effluent, and v_0 is the feed flow rate, which may be written as:

$$v_0 = \frac{V}{\mathrm{HRT}} \tag{2}$$

where, V is the theoretical working volume of PABR. Eqs.(1) and (2) give:

$$\frac{M}{V} = \int_0^\infty C_A \mathrm{d}(\frac{t}{\mathrm{HRT}}) \tag{3}$$

Eq. (3) can be rearranged as:

$$\int_0^\infty C\mathrm{d}\theta = 1 \tag{4}$$

where,

$$C = \frac{C_A}{M/V} \tag{5}$$

and

$$\theta = \frac{t(\mathrm{h})}{\mathrm{HRT(h)}} \tag{6}$$

Equations (5) and (6) provide the expression of normalized concentration (C) and normalized time (θ) affording facilities for comparison between RTD studies.

The typical C-curves (C vs.θ) thus obtained are shown in Figs.2c, 3c, and 4c. These curves were then analyzed further using a model derived from Levenspiel (1972), as the programme calculated the mean (μ_t) and variance (σ_t) of the curve, the fraction of dead space in the reactor (V_d/V), the overall dispersion number ($D/\mu L$), and the equivalence number of equal-sized ideal stirred tanks in series (N). The calculation methods are given below, and the results for all runs are summarized in Table 2.

Table 2 Results of the RTD studies

Run no.	μ_t	$\frac{V_d}{V}$ (%)	σ_t^2	N	$\frac{D}{\mu L}$	Lithium recovery (%)
a(1)	0.9463	7.57	0.1443	6.93	0.0783	103.38
a(2)	0.8935	20.68	0.1659	6.03	0.0913	99.70
a(3)	0.8943	16.65	0.1566	6.38	0.0856	100.71
b(1)	0.9672	4.61	0.1545	6.47	0.0844	103.62
b(2)	0.9549	19.48	0.1842	5.43	0.1026	97.87
b(3)	0.9421	16.32	0.2306	4.34	0.1330	99.30
c(1)	0.8662	9.11	0.1399	7.15	0.0757	96.34
c(2)	0.8239	23.88	0.1667	6.00	0.0918	95.34
c(3)	0.8317	18.35	0.1627	6.15	0.0893	95.45

The cut-off point for the "tail" was taken at θ=2, as in Levenspiel's model. The area under the cover between $\theta = 0$ and $\theta = 2$ represents the fraction of Li^+ recovered within 2 HRTs (v_a), while the total area under the C-curve is unity. Therefore, the mean of the curve is given by:

$$\mu_t = \frac{\int_0^2 x \times f(x)\mathrm{d}x}{\int_0^2 f(x)\mathrm{d}x} \tag{7}$$

and the variance of the curve can be expressed as:

$$\sigma_t^2 = \frac{\int_0^2 (x-\mu)^2 \times f(x)\mathrm{d}x}{\int_0^2 f(x)\mathrm{d}x} \tag{8}$$

The fraction of dead space is then given by:

$$\frac{V_d}{V} = 1 - v_a \times \mu_n \tag{9}$$

where, V_d is the volume of dead space in the reactor. In a tanks-in-series model,

$$\sigma_t^2 = \frac{1}{N} \tag{10}$$

also, in a dispersion model,

$$\sigma_t^2 = 2(\frac{D}{\mu L}) - 2(\frac{D}{\mu L})^2 \times (1 - e^{-\frac{\mu L}{D}}) \tag{11}$$

From the above equations, it can be noted that the calculation of dead space is associated with the mean of the

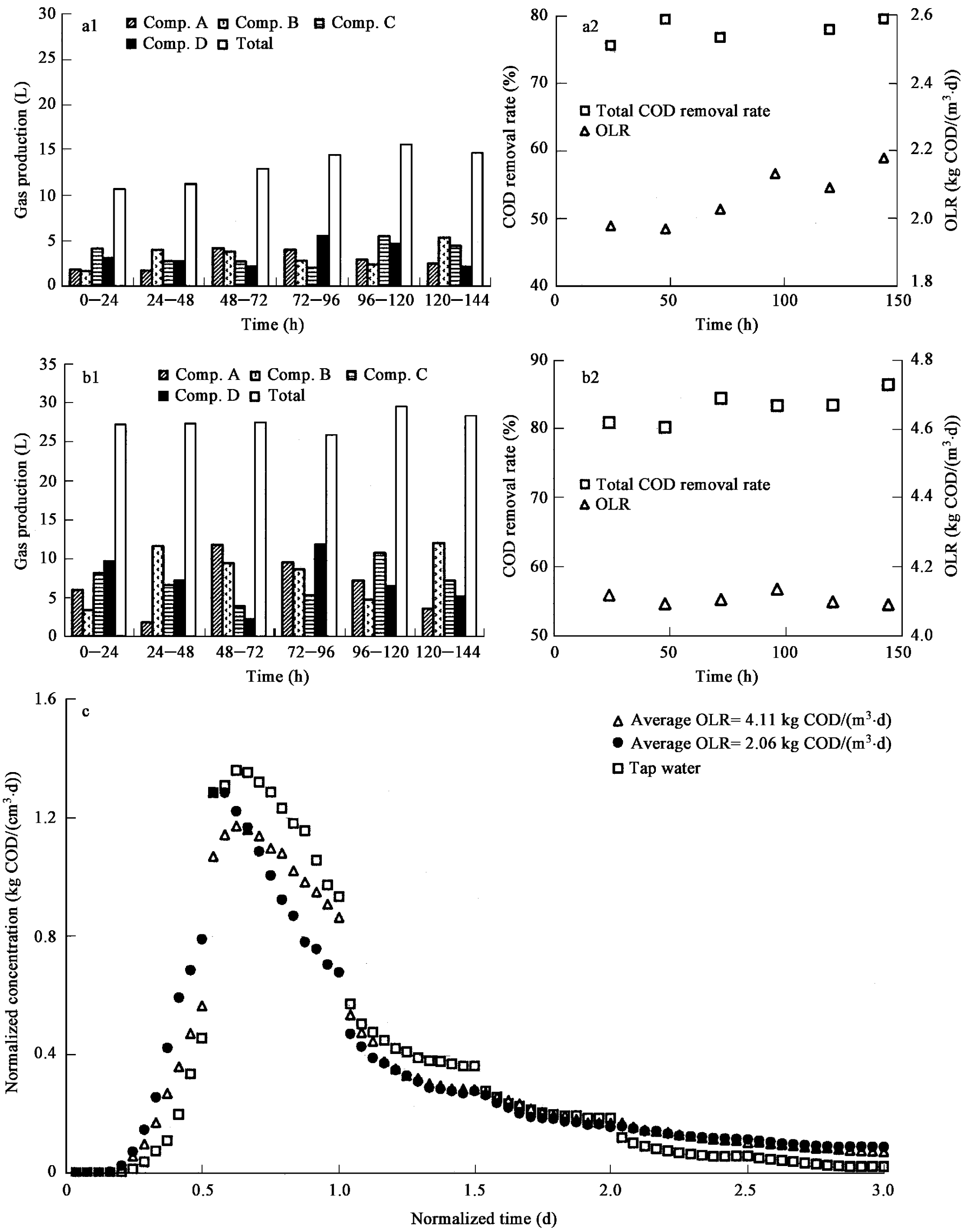

Fig. 2 RTDs of PABR operated at the stable periodic state with T = 4 d and HRT = 2 d in a "clockwise sequential" switching manner at different OLRs (Run a (1, 2, 3)). (a) variation of gas production, OLR, and total COD removal rate in the RTD of average OLR=2.06 kg COD/(m^3·d); (b) variation of gas production, OLR, and total COD removal rate in the RTD of average OLR=4.11 kg COD/(m^3·d); (c) C-curves of PABR at different OLRs.

curve, while the dispersion or back-mixing is associated with the variance.

The programme was performed in Matlab Release 14 with Service Pack 3 (R14SP3) (Minitab Inc., USA). Cubic polynomial curve fittings, whose accuracy depends largely on the spacing of the points on the curve, were done on intervals of $\theta \in [0, 0.5]$, (0.5, 1), (1, 1.5), (1.5, 2), (2, 2.5), and (2.5, 3), respectively. Points were interpolated linearly until the adjusted R-square statistic obtained on the fittings increased above 0.99. Integration under the curve was then achieved based on the results from the fittings. Finally, the calculations of μ_t, σ_t, V_d/V, $D/\mu L$, N, and Lithium recovery (%) were all completed. Although the programme took different approaches in the mathematical analysis, the mass balances performed on Li^+ showed agreement ranging between 95.34 and 103.62% (Table 2) between the mass injected and the mass detected in the effluent over time, which agreed with the previous studies (Grobicki and Stuckey, 1992; Langenhoff *et al.*, 2000; Langenhoff and Stuckey, 2000).

2.1 Dead space

It should be noted that the calculated values of dead space in PABR were low by comparison with the studies of

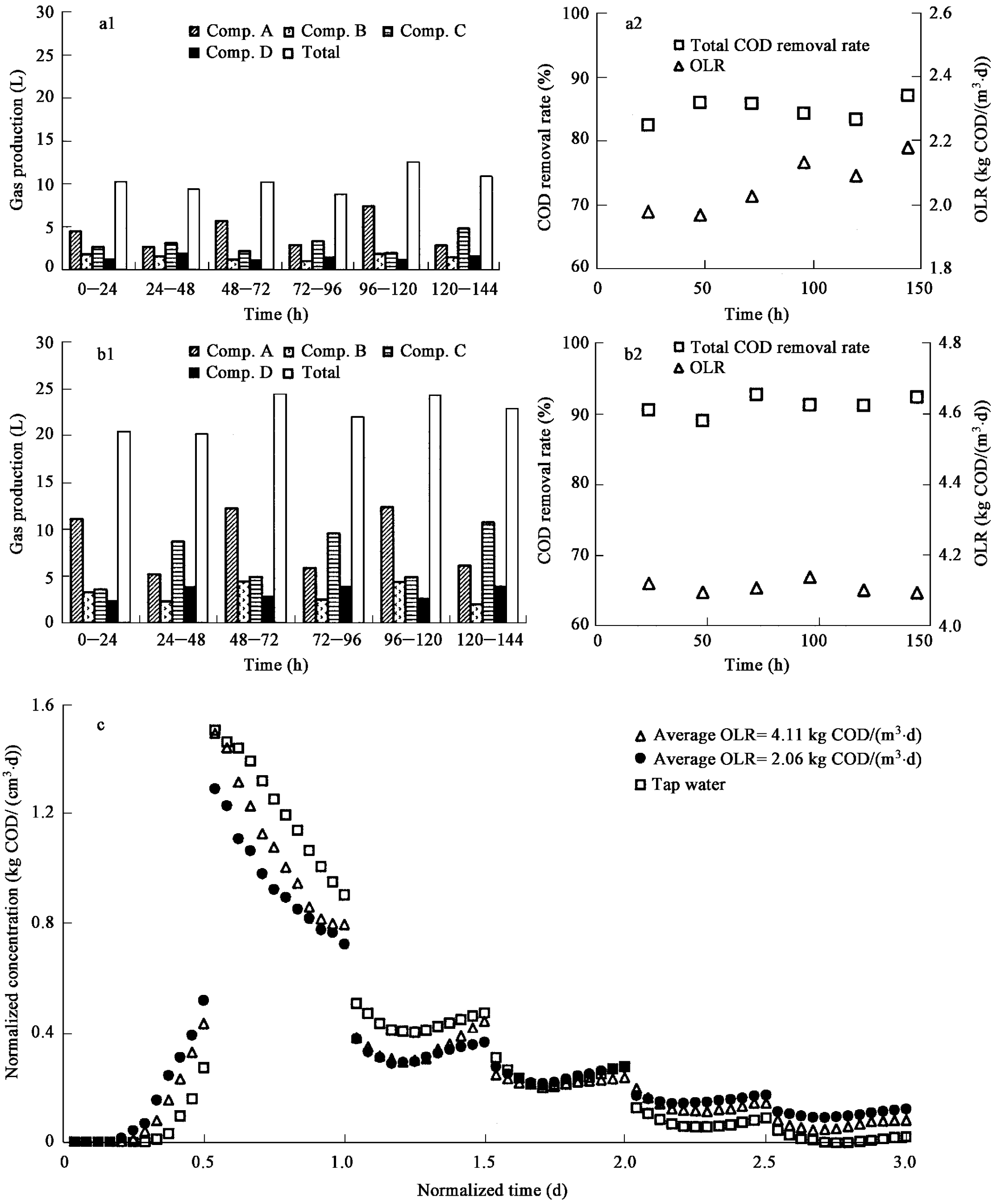

Fig. 3 RTDs of PABR operated at the stable periodic state with T = 2 d and HRT = 2 d in an "every second" switching manner at different OLRs (Run b (1, 2, 3)). (a) variation of gas production, OLR, and total COD removal rate in the RTD of average OLR=2.06 kg COD/(m^3·d). (b) variation of gas production, OLR, and total COD removal rate in the RTD of average OLR=4.11 kg COD/(m^3·d); (c) C-curves of PABR at different OLRs.

other reactors, which was the same as the results obtained in ABR by Grobicki and Stuckey (1992). In physical terms, dead space may be divided into the categories of biological dead space and hydraulic dead space (Young and Young, 1988), with hydraulic dead space a function of the flow rate and the number of compartments in the reactor and biological dead space a function of the biomass concentration and activity (Grobicki and Stuckey, 1992).

Hydraulic dead space tends to occur beneath weirs and in corners, where stagnant eddies form. The eddies effectively act as reservoirs, into and out of which the tracer slowly diffuses. On the C-curve, this appears as a smooth tail: the larger the hydraulic dead space, the greater is the area of the tail. Clearly, in the runs without biomass (Run a(1), b(1), c(1)), the dead space were all hydraulic dead space. A comparison among the tap water C-curves in Figs.2c, 3c, and 4c at the same HRT of 2 d showed that the tap water C-curve in an "every second" switching manner with T = 2 d has the smallest area of the tail corresponding to the lowest calculated value of dead space and the highest peak of normalized concentration whereas that in a T = ∞ (ABR) switching manner has the greatest area of the tail corresponding to the highest calculated value of dead space and the lowest peak of normalized concentration. These results were mainly because of the difference in the switching manners besides stagnant eddies forming

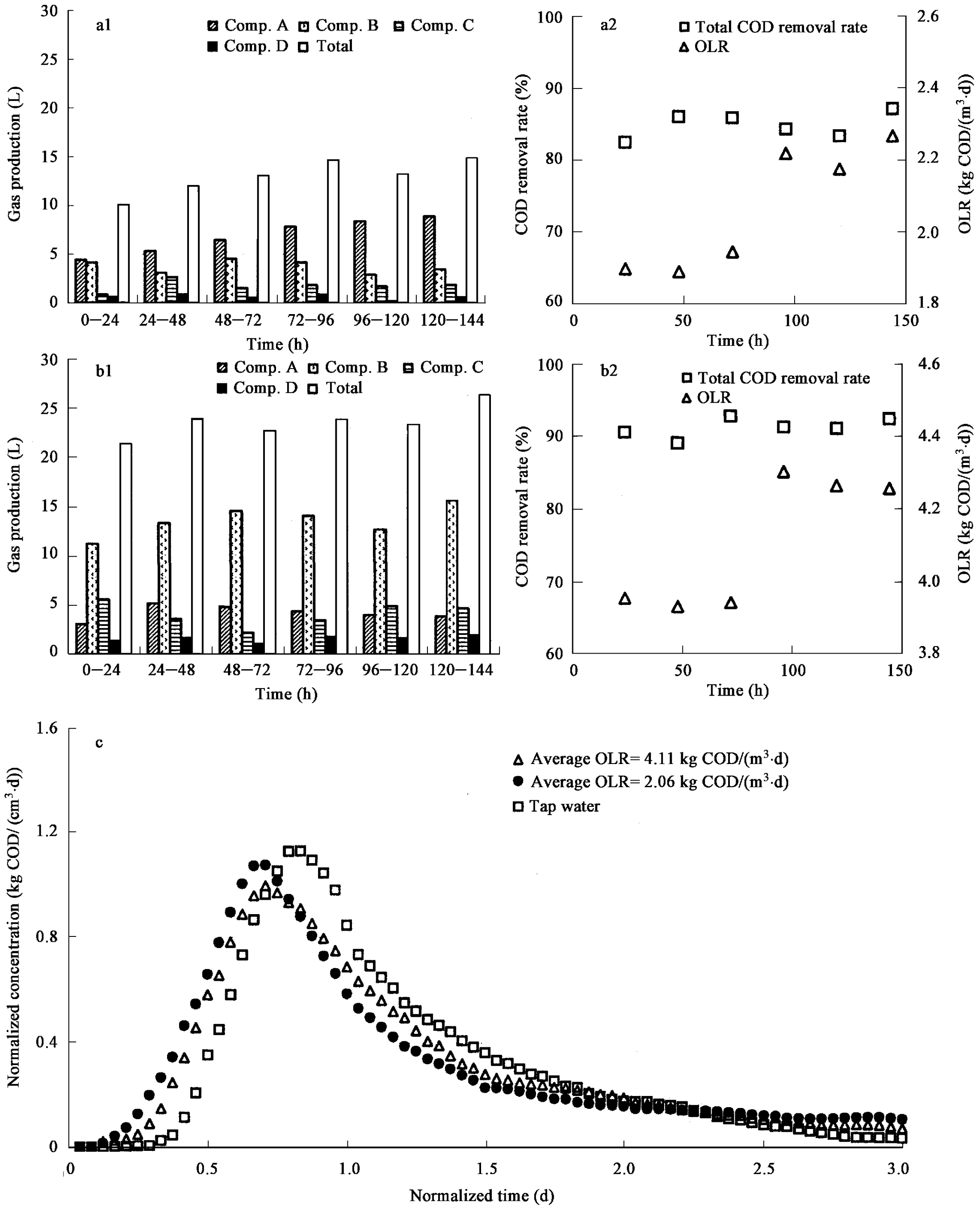

Fig. 4 RTDs of PABR operated at the stable periodic state with $T = \infty$ (ABR) and HRT = 2 d at different OLRs (Run c (1, 2, 3)). (a) variation of gas production, OLR, and total COD removal rate in the RTD of average OLR=2.06 kg COD/(m^3·d); (b) variation of gas production, OLR, and total COD removal rate in the RTD of average OLR=4.11 kg COD/(m^3·d); (c) *C*-curves of PABR at different OLRs.

beneath weirs and in corners, and tracer diffused into effluent most quickly in an "every second" switching manner with $T = 2$ d and most slowly in a $T = \infty$ (ABR) switching manner.

Biological dead space is the volume occupied by the biomass, together with the dead space caused by the interference of biomass particles in flow patterns (i.e., the stagnant liquid layer around the particles). Run a(2), b(2), c(2) and Run a(3), b(3), c(3) were performed with the average OLR at about 2 and 4 kgCOD/(m^3·d), respectively, and thus, both biological and hydraulic dead space contributed to the total dead space. It can be seen from the *C*-curves in Figs.2c, 3c, and 4c with the average OLR at about 2 and 4 kgCOD/(m^3·d) that the initial difference in the biomass in the reactors did not influence the percentage of dead space in the reactors, because no quantitative difference could be observed between the three reactors. No matter what the OLR was, the total dead space in the PABR run in an "every second" switching manner with $T = 2$ d was the lowest whereas that in the PABR run in a $T = \infty$ (ABR) switching manner was the highest. By increasing the OLR, a higher gas production took place in each compartment as the COD removal efficiency increased (Figs.2(a, b), 3(a, b), 4(a, b), and Table 1). The rapid evolution of gas bubbles and the greater degree of fluidization of the granules or flocs to a large extent prevented the formation of channels through the bed. Hence, more mixing in the reactor occurs, thus creating less (biological) dead space, or at least counterbalancing the increase in hydraulic dead space in the reactor caused by channeling. Biological dead space was also to some extent a stagnant area that might act as a reservoir for the tracer, thus contributing to tailing. Therefore, whichever switching manner the PABR run in, the *C*-curves at different average OLRs showed the same trend that biological dead space was the major contributor to dead space at HRT of 2 d but affected decreasingly at higher OLR: the larger the total dead space, the greater the area of the tail.

Hydraulic dead space has been shown to increase with increasing Reynolds (Young and Young, 1988), and thus, this effect will become more important at low HRT. Langenhoff and Stuckey (2000) suggested that the volume of dead space of ABR was relatively constant at different temperatures, even though less gas was produced at low temperature owing to the lower COD removals. Thus, more experiments should be run in PABR to see if any conclusions may be drawn at various HRTs in diverse switching manners and frequencies at different temperatures.

2.2 Mixing patterns

Mixing patterns are analyzed largely by observing the variance of the *C*-curve, and fitting this information into the tanks-in-series model and the dispersion model.

Tomlinson and Chambers (1979) defined $D/\mu L$ =0.02 as an "intermediate" degree of dispersion and $D/\mu L$ = 0.2 as "large" (An ideal perfectly mixed reactor would show $D/\mu L = \infty$, while ideal plug flow would show $D/\mu L$ = 0). Using the calculated dispersion numbers in the PABRs (Table 2), it could be concluded that the flow patterns within the PABRs were intermediate between plug-flow and perfectly mixed under all the conditions tested.

The RTD studies of ABR done by Grobicki and Stuckey (1992) showed that ABR might be represented for the purposes of modeling as a series of ideal stirred tanks, corresponding to the number of acrual compartments. Also, at low HRT (below 20 h), the lower the HRT, the better N alone fitted the number of actual compartments. The values of N showed in Table 2 were all greater than the number of actual compartments because all runs were performed at high HRT of 2 d.

3 Conclusions

The fraction of dead space in PABR was similar to that in ABR, which was low in comparison with other reactor designs. Dead space may be divided into two categories, hydraulic and biological. In RTD studies without biomass at the same HRT of 2 d, the hydraulic dead space in the PABR run in an "every second" switching manner with T = 2 d was the lowest while that in the PABR run in a $T = \infty$ (ABR) switching manner was the highest. The same trend was obtained with the total dead space in RTD studies with biomass at HRT of 2 d no matter what the OLR was. Biological dead space was the major contributor to dead space but affected decreasingly at higher OLR whichever switching manner the PABR run in.

The flow patterns within the PABRs were intermediate between plug-flow and perfectly mixed under all the conditions tested.

References

American Public Health Association, 1995. Standard methods for examination of water and wastewater[S]. 19th ed. American Public Health Association, Washington, DC.

Grobicki A, Stuckey D C, 1992. Hydrodynamic characteristics of the anaerobic baffled reactor[J]. Water Research, 26(3): 371–378.

Langenhoff A A M, Intrachandra N, Stuckey D C, 2000. Treatment of dilute soluble and colloidal wastewater using an anaerobic baffled reactor: influence of hydraulic retention time[J]. Water Research, 34(4): 1307–1317.

Langenhoff A A M, Stuckey D C, 2000. Treatment of dilute wastewater using an anaerobic baffled reactor: effect of low temperature[J]. Water Research, 34(15): 3867–3875.

Levenspiel O, 1972. Chemical reaction engineering[M]. 2nd ed. New York: Wiley. 253–308.

Skiadas I V, Lyberatos G, 1998. The periodic anaerobic baffled reactor[J]. Water Science Technology, 38(8/9): 401–408.

Skiadas I V, Gavala H N, Lyberatos G, 2000. Modelling of the periodic anaerobic baffled reactor (PABR) based on the retaining factor concept[J]. Water Research, 34(15): 3725–3736.

Stamatelatou K, Lyberatos G, 2002. Simulation of a periodic anaerobic baffled reactor (PABR): steady state and dynamic response[J]. Water Science and Technology, 45: 81–86.

Stamatelatou K, Vavilin V, Lyberatos G, 2003. Performance of a glucose fed periodic anaerobic baffled reactor (PABR) under increasing organic loading conditions: 1. experimental results[J]. Bioresource Technolology, 88: 131–136.

Stamatelatou K, Skiadas I V, Lyberatos G, 2004. On the behavior of the periodic anaerobic baffled reactor (PABR) during the transition from carbohydrate to protein-based feedings[J]. Bioresource Technology, 92: 321–326.

Tomlinson E J, Chambers B, 1979. The effect of longitudinal mixing on the settleability of activated sludge[R]. Technical Report TR 122, Water Research Centre, Stevenage.

Young H W, Young J C, 1988. Hydraulic characteristics of upflow anaerobic filter[J]. Journal of Environment Engineering, 114: 621–638.